© 2022. Published by The Company of Biologists Ltd | Journal of Cell Science (2022) 135, jcs259375. doi:10.1242/jcs.259375

RESEARCH ARTICLE

MAPK activation drives male and female mouse teratocarcinomas from late primordial germ cells

Eugenia Guida[1,§], Valentina Tassinari[1,*,§], Ambra Colopi[1], Federica Todaro[1], Valeriana Cesarini[1,‡], Benedetto Jannini[1], Manuela Pellegrini[2], Flavia Botti[3,4], Gabriele Rossi[1], Pellegrino Rossi[1], Emmanuele A. Jannini[5] and Susanna Dolci[1,¶]

ABSTRACT

Germ cell tumors (GCTs) are rare tumors that can develop in both sexes, peaking in adolescents. To understand the mechanisms that underlie germ cell transformation, we established a GCT mouse model carrying a germ-cell-specific *BRaf*^{V600E} mutation with or without heterozygous *Pten* deletion. Both male and female mice developed monolateral teratocarcinomas containing embryonal carcinoma (EC) cells that showed an aggressive phenotype and metastatic ability. Germ cell transformation started in fetal gonads and progressed after birth leading to gonadal invasion. Early postnatal testes showed foci of tumor transformation, whereas ovaries showed increased number of follicles, multi-ovular follicles (MOFs) and scattered metaphase I oocytes containing follicles. Our results indicate that MAPK (herein referring to Erk1/2) overactivation in fetal germ cells of both sexes can expand their proliferative window leading to neoplastic transformation and metastatic behavior.

KEY WORDS: BRaf V600E, Teratocarcinoma, Germ cells, Ovary, Testis

INTRODUCTION

Human germ cell tumors (hGCTs) represent a model of progressive neoplastic transformation starting from primordial germ cells (PGCs) or from more developmentally advanced germ cells, such as gonocytes (i.e. the male or female fetal gonadal germ cells). Whereas female GCTs occur mainly in neonates, infants and adolescents, and rarely in the adults, male GCTs mainly peak during early adulthood, ∼30–35 years (Feldman et al., 2013). They arise primarily in ovaries or in testes, although they can also occur less frequently in extragonadal sites (De Felici et al., 2021). GCTs account for ∼98% of testicular cancer cases (testicular germ cell tumors, TGCTs) (Bosl and Motzer, 1997) and for only 2–3% of ovarian cancer cases (ovarian germ cell tumors, OGCTs) (Permuth-Wey and Sellers, 2009; De Felici and Dolci, 2013; Dolci et al., 2015; Quirk et al., 2005).

Germ cell development is a tuned process that starts early during embryogenesis, and it dictates the reproductive cycle of an individual. Faulty epigenetic remodeling, unrestricted proliferation, and defects in apoptosis or in meiotic commitment can be all potential drivers of germ cell neoplastic transformation during gametogenesis. The unique characteristics of such processes in the germline and the latent pluripotency of PGCs and gonocytes make these cells prone to cell transformation and can be at the basis of the multiform aspects of GCTs. Human TGCTs have recently been classified into two groups: tumors originating from a pre-existing *in situ* lesion, defined as germ cell neoplasia *in situ* (GCNIS, type I), and tumors that develop independently from GCNIS (type II) (Moch et al., 2016). Those originating from GCNIS occur after puberty in young males (Reuter, 2005; Skakkebaek et al., 1987) and can potentially derive from PGCs or fetal/neonatal gonocytes (Depue et al., 1983; Sonne et al., 2009). Two cancer forms can originate from GCNIS, seminomas (SE) or non-seminomas (non-SE) or even a mixed form, that can display markers of both fetal germ cells and pluripotency (Rajpert-De Meyts, 2006). SEs are less aggressive compared to non-SEs, that include tumors with different malignancy grades and histological components such as embryonal carcinoma (EC), trophoblastic tumors (TTs), post-pubertal yolk sac tumors (YSTs), post-pubertal teratomas (TEs), and teratomas with somatic type malignancy. The GCT class unrelated to GCNIS includes spermatocytic tumors (STs), which are thought to originate from spermatogonia or spermatocytes, pre-pubertal YSTs, pre-pubertal TEs and mixed pre-pubertal TEs and YSTs (Moch et al., 2016). They are rare and self-limiting and typical of elderly men (Oosterhuis and Looijenga, 2005). Gonadoblastomas are considered the GCNIS counterpart of the fetal ovaries at the origin of the OGCT, and can develop as dysgerminomas (DG, the most common type, histologically similar to SE) or non-dysgerminomas (non-DG, similar to non-SE). The most common types of non-DG are YSTs, immature TEs, and mixed GCTs, with less common variants including ECs, polyembryomas and non-gestational choriocarcinomas (Gershenson, 2007). To understand the mechanisms underlying germ cell transformation, mouse genetic models for GCTs have been assessed, such as heterozygosity for mutated Kit ligand (*KL*; also known as *Kitlg*), and Dead-end (*Dnd1*)-, *Pten*- and *Dmrt1*-knockout mice (Kimura et al., 2003; Krentz et al., 2009; Stevens, 1964; Youngren et al., 2005); however, all of them develop only TEs, directly from transformed early PGCs and mostly in males and none of them show GCNIS lesions preceding the tumor lesions. Mice overexpressing Gdnf, the Ret-Gfra1 ligand, form non-metastatic SEs similar to ST (Meng et al., 2001). Recently, a

[1]Department of Biomedicine and Prevention, University of Rome Tor Vergata, Rome, Italy. [2]Institute of Biochemistry and Cell Biology, IBBC-CNR, Monterotondo, Rome, Italy. [3]Department of Experimental Medicine, University of Rome Tor Vergata, Rome, Italy. [4]Pathology Department, S. Eugenio Hospital, Rome, Italy. [5]Department of Systems Medicine, University of Rome Tor Vergata, Rome, Italy. *Present address: Department of Molecular Medicine, 'Sapienza' University of Rome, Rome, Italy. ‡Present address: Department of Biomedical Sciences, Institute of Translational Pharmacology, CNR, Rome, Italy
§These authors contributed equally to this work

¶Author for correspondence (dolci@uniroma2.it)

E.G., 0000-0002-1690-3277; V.T., 0000-0003-2167-9414; A.C., 0000-0003-1581-0527; V.C., 0000-0001-9323-1796; B.J., 0000-0002-5266-2706; M.P., 0000-0001-6387-5187; F.B., 0000-0002-7266-1014; P.R., 0000-0003-4796-327X; S.D., 0000-0002-6864-3673

Handling Editor: Caroline Hill
Received 15 September 2021; Accepted 9 March 2022

Journal of Cell Science (2022) 135, jcs259375. doi:10.1242/jcs.259375

gonocyte *Pten*^{del} *KRas*^{G12V} mutant model has been produced that develops testicular ECs resembling type I GCT, that evolve without GCNIS lesions (Pierpont et al., 2017).

To understand if either male or female early meiotic germ cells could behave as cell of origin of GCTs, we produced a mouse model in which *Pten* deletion was specifically induced through the early meiotic and male germ cells deleter *Spo11*^{Cre} (Pellegrini et al., 2011). To over-activate the germ cell mitogen-activated protein kinase [MAPK; herein referring to Erk1 and Erk2 (Erk1/2, also known as MAPK3 and MAPK1, respectively)] pathway, we inserted a *BRaf*^{V600E} mutated allele that was activatable by Cre recombination (Honecker et al., 2009; Meintker et al., 2020).

Such a mutation, although rare in hGCTs, has been identified in cisplatin-resistant gonadal or extragonadal TGCTs and successfully targeted by treatment with vemurafenib, the specific *BRaf*^{V600E} inhibitor (Boublikova et al., 2016; Feldman et al., 2014; Sommerer et al., 2005). We found that in ∼30% male and in 30% female gonads in which the MAPK pathway was activated, ECs were equally induced. As with human ECs, both testicular and ovarian GCTs stained for EC markers such as Oct4 (also known as Pou5f1), Sox2, Prdm14 and AP2γ (also known as Tfap2c), indicating that these cells are pluripotent. In females, non-tumoral ovaries from *Spo11*^{Cre} *Pten*$^{+/flox}$ *Braf*^{V600E} or from *Spo11*^{Cre} *Braf*^{V600E} animals showed increased amounts of primordial, growing and multi-ovular follicles (MOFs), as well as metaphase I oocytes. Altogether, these results suggest that dysregulation of MAPK signaling can lead to transformation of fetal germ cell and to anomalies of postnatal germ cell development.

RESULTS

Constitutive MAPK activation in late PGCs induces testicular and ovarian tumors in postnatal mice

Mice heterozygous for *Pten* deletion (*Pten*$^{+/-}$) are prone to developing different types of tumors, including testicular TEs late in adulthood (Suzuki et al., 1998), whereas deletion of both *Pten* alleles in early PGCs leads to TE formation in neonatal mice. Recently, homozygous deletion of *Pten* and concomitant addition of *KRas*^{G12V} mutation in PGCs has been shown to induce EC formation in pre-puberal mice (Pierpont et al., 2017). We wondered whether early meiotic germ cells could also be susceptible to undergoing malignant transformation. To this end, we employed the germ cell specific *Spo11*^{Cre} deleter, which we have previously shown to be active in early spermatocytes and oocytes at meiotic entry (Pellegrini et al., 2011). *Spo11*^{Cre} *Pten*$^{+/flox}$ compound mutants did not show any overt phenotype; however, we never succeeded in obtaining *Spo11*^{Cre} *Pten*$^{-/flox}$ compound mutants, suggesting that Spo11^{Cre} activity was also present ectopically, causing embryonic loss. Whole-mount β-galactosidase staining (β-gal) of 13.5 days post coitum (dpc) *Spo11*^{Cre}, *LacZ-R26*$^{flox/flox}$ embryos revealed that skin hair and vibrissae follicles, as well as forebrain regions, expressed LacZ as a readout of Spo11^{Cre} transgene activity (Fig. S1A,B), suggesting that *Spo11*^{Cre}-mediated *Pten* homozygous deletion occurred ectopically, leading to embryonic lethality. Given that MAPK pathway activation stimulates spermatogonia proliferation (Dolci et al., 2001; Tassinari et al., 2015), we included the *BRaf*^{V600E} inducible mutation to over-activate MAPK pathway in the *Spo11*^{Cre} *Pten*$^{+/flox}$ background. To this end, we obtained *Spo11*^{Cre} *Pten*$^{+/flox}$ *BRaf*^{V600E}, *Spo11*^{Cre} *Pten*$^{+/flox}$ or *Spo11*^{Cre} *BRaf*^{V600E} compound mutants along with *Spo11*^{Cre} negative genotypes, which were all considered as controls. All the assorted genotypes were delivered with a mendelian frequency. Owing to Spo11^{Cre} ectopic activity the presence of *BRaf*^{V600E} allele either in *Pten*^{wt} (*wt*, wild-type) or in *Pten*$^{+/flox}$ backgrounds induced hyperkeratosis (Fig. S1C,D) and neurological defects in the pups, which did not survive beyond 25 days post-partum (dpp), indicating that constitutive MAPK pathway activation in the neural and/or in other tissues was lethal.

At time of killing (25 dpp), ∼30% of *Spo11*^{Cre} *Pten*$^{+/flox}$ *BRaf*^{V600E} showed a monolateral mass that replaced most of the gonad, both in male and in female animals (33% males and 28.5% females; Table S1) (Fig. 1A,B). At a lower, although significant, percentage (27%), compared to the *BRaf*^{V600E} *Pten*^{wt} genotype tumor formation occurred also in *Spo11*^{Cre} *BRaf*^{V600E}-only genotype, suggesting that the BRaf-Mek-MAPK pathway is linked to germ cell transformation (Table S1). Since the tumor mass was evident at the time of killing in both sexes, it was unlikely that oncogene activation occurred at meiotic entry, at least in males. Indeed, Pierpont et al. (Pierpont et al., 2017) have recently shown that when using the premeiotic *Stra8*^{Cre} deleter, Cre expression preceded that of endogenous *Stra8* at earlier stages in PGCs. Thus, we performed a detailed analysis of Spo11^{Cre} activity in fetal and postnatal gonads to follow the correct timing of transgene expression.

Spo11^{Cre} activity was detectable in male germ cells at 7 dpp, when premeiotic and pre-leptotene spermatocytes are present, but at 18.5 dpc only a few tubules per testis contained β-gal-positive gonocytes (Fig. 1C). To find out whether Spo11^{Cre} activity was present at earlier stages of fetal germ cell development, we employed *Eyfp-R26*$^{flox/flox}$ mice, which offered a more sensitive identification assay for the recombinase activity. We found that only one out of four Spo^{Cre}-positive 12.5 dpc male embryos contained small clusters of Eyfp-positive gonocytes within the seminiferous tubules (Fig. 1C). In females, the majority of oocytes at different stages of development (18 dpc, 12 and 25 dpp) showed positive β-gal staining, including mis-localized oocytes within the mesovarium (25 dpp) (Fig. 1D) (Pellegrini et al., 2011). As observed in males, EYFP expression was found only in few oogonia (one out of three) of 12.5 Cre-positive ovaries confirming that Spo11^{Cre} activity occurred before meiotic entry both in male and female germ cells (Fig. 1D). Overall, these results indicated that Spo11-driven Cre expression occurred ectopically in few late PGCs of both sexes and that BRaf^{V600E} editing in proliferating germ cells was sufficient to induce their transformation. This latter event means it is unlikely that the incomplete penetrance of the tumor phenotype was due to loss of *Pten* heterozygosity.

Gonadal teratomas contain EC cells

Analysis of the histology of *BRaf*^{V600E}-mutated tumors revealed the presence of teratomatous tissue that contained several islands of undifferentiated cells resembling malignant EC cells both in female and male tumors (Fig. 2A,C). Immuno-histochemical analysis of the gonadal lesions showed nests of cells expressing the stem cell markers Oct4, Sox2, AP2γ and Prdm14 (Fig. 2B; Fig. S2A) and staining with anti-Ki67 (also known as Mki67) antibody detected high levels of proliferative activity within the nests (more than 90% Ki67-positive cells, Fig. 2B) whereas the differentiated counterpart showed a low proliferation index (less than 1%, data not shown). By histology and immuno-histochemistry analysis, we found that mouse tumors were similar to human ECs but not to SEs, as revealed by differential Sox2 and Prdm14 immunostaining (Fig. 2D). Western blot analysis showed that tumors from both sexes expressed Kit, Sox2, Oct4 and Prdm14, confirming that female and male teratocarcinomas originated from germ cells and contained EC cells (Fig. 2E). In two out of 39 *Spo11*^{Cre} *Pten*$^{+/flox}$ *BRaf*^{V600E} mice, we found intestinal metastases that diffused by contiguity from the gonadal site and were characterized by differentiated and poorly differentiated tumor cells (Fig. 2F). In two

Journal of Cell Science (2022) 135, jcs259375. doi:10.1242/jcs.259375

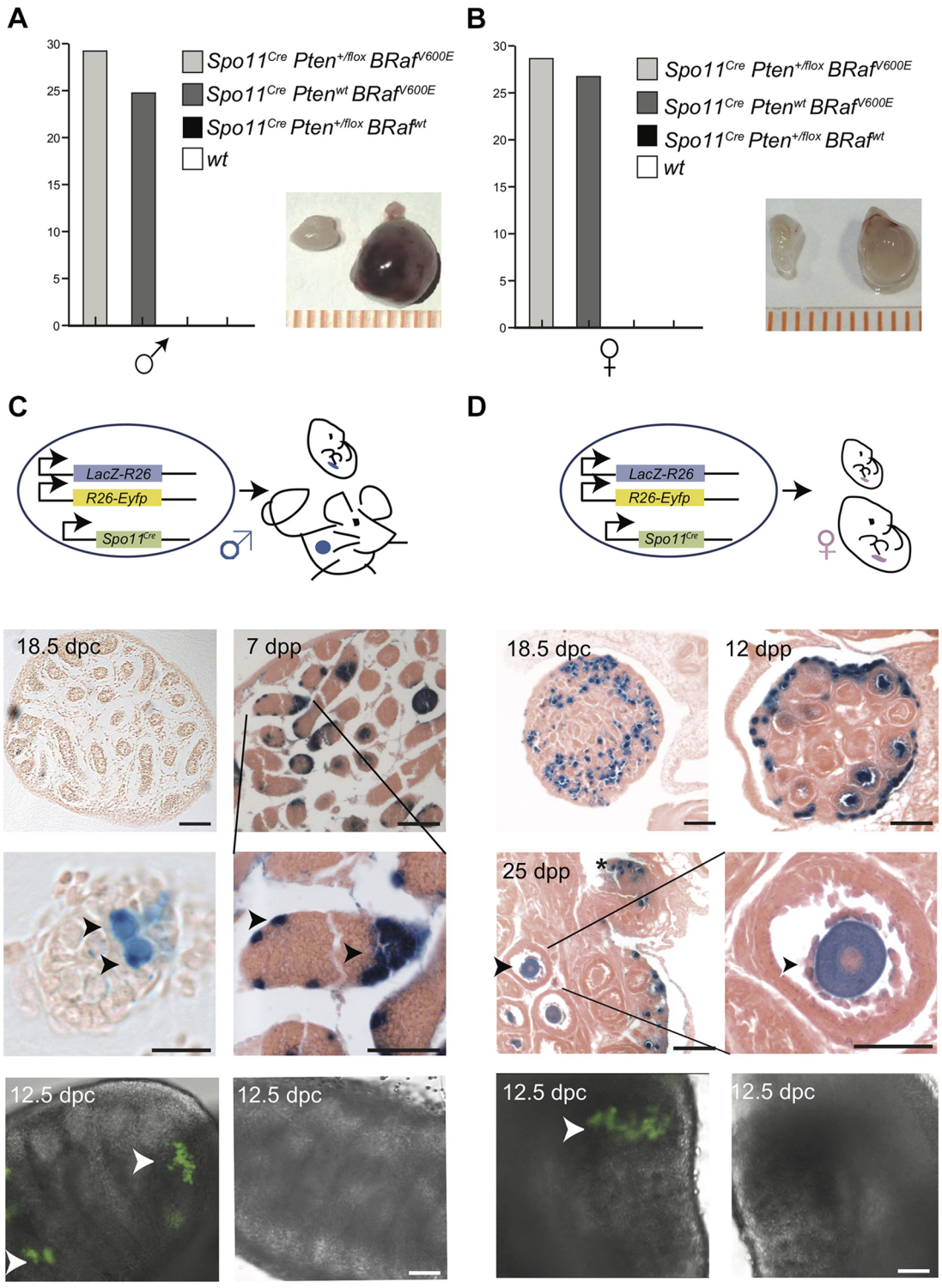

Fig. 1. GCTs in Spo11^{Cre} *BRaf^{V600E}* male and female postnatal gonads. (A) Incidence of tumors occurrence (expressed in percentage) in male *Spo11^{Cre} Pten$^{+/flox}$ BRaf^{V600E}*, *Spo11^{Cre} Pten^{wt} BRaf^{V600E}*, *Spo11^{Cre} Pten$^{+/flox}$ BRaf^{wt}* and *wt* control mice at 25 dpp, with representative images of *Spo11^{Cre} Pten$^{+/flox}$ BRaf^{V600E}* tumors versus wt gonads (*n*=18). (B) Incidence of tumors occurrence in female *Spo11^{Cre} Pten$^{+/flox}$ BRaf^{V600E}*, *Spo11^{Cre} Pten^{wt} BRaf^{V600E}*, *Spo11^{Cre} Pten$^{+/flox}$ BRaf^{wt}* and *wt* control mice at 25 dpp, with representative images of *Spo11^{Cre} Pten$^{+/flox}$ BRaf^{V600E}* tumors versus wt gonads (*n*=21). In A,B, black and white bars are too small to show. (C) Top, schematic representation of Spo11^{Cre} editing in male mice. Underneath are representative gonadal sections to reveal Spo11^{Cre} activity by β-gal staining in *Spo11^{Cre} LacZ-R26* testes at 18.5 dpc and 7 dpp (top and middle) and EYFP detection in *Spo11Cre Eyfp-R26* testes at 12.5 dpc (bottom) versus *wt*. Scale bars: 50 µm (*n*=4). Black arrowheads point to β-gal-positive gonocytes and spermatogonia (middle left and middle right panels, respectively). White arrowheads point to EYFP positive late PGCs within fetal testicular cords (bottom left panel). (D) Top, schematic representation of Spo11^{Cre} editing in female mice. Underneath are representative gonadal sections to reveal Spo11^{Cre} activity by β-gal staining in *Spo11^{Cre} LacZ-R26* ovaries at 18.5 dpc, 12 and 25 dpp (top and middle) and EYFP detection in *Spo11Cre Eyfp-R26* ovaries at 12.5 dpc (bottom) versus *wt*. Scale bars: 50 µm (*n*=3). Black arrowheads point to β-gal-positive growing follicle-enclosed oocytes (left and right middle panels); the asterisk indicates mislocated oocytes within the mesovarium (left middle panel). White arrowheads point to EYFP-positive late PGCs within the fetal ovary (bottom left panel).

Journal of Cell Science

Journal of Cell Science (2022) 135, jcs259375. doi:10.1242/jcs.259375

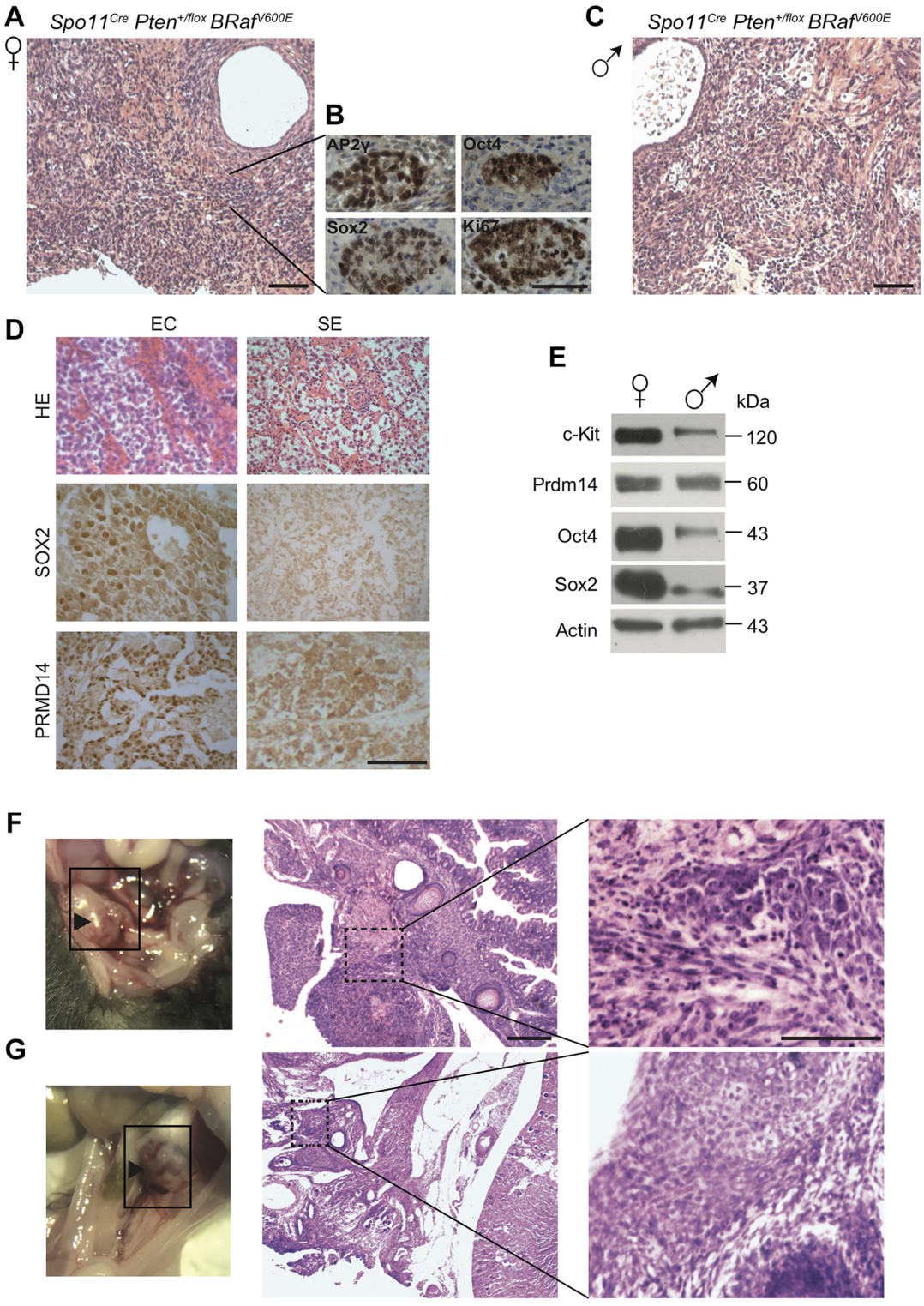

Fig. 2. *BRaf*^{V600E} edited female and male germ cells develop teratocarcinomas. (A) H&E-stained sections of *Spo11*^{Cre} *Pten*$^{+/flox}$ *BRaf*^{V600E} female tumors (*n*=4). Scale bar: 50 µm. (B) Immunohistochemical analysis of lesions probed with AP2γ, Oct4, Sox2 and Ki67 on gonadal tumors (*n*=5). Scale bar: 100 µm. (C) H&E-stained sections of *Spo11*^{Cre} *Pten*$^{+/flox}$ *BRaf*^{V600E} male tumors (*n*=4). Scale bar: 50 µm. (D) Histological and immunohistochemical analysis of human embryonal carcinoma and seminoma sections, stained with HE and probed for SOX2 and PRDM14 (*n*=3). Scale bar: 50 µm. (E) Western blot analysis on tumor tissue extracts probed for Kit, Prdm14, Oct4 and Sox2. Actin was used as a reference gene (*n*=3). (F) Localization and histological analysis of an intestinal metastasis. Left image shows the tumor mass in the abdominal cavity. The square identifies the intestinal area of tumor invasion and arrow points to the tumor. Middle panel shows a histological preparation of the tumor, invading the intestinal wall. Dashed square points to a representative enlarged area showing differentiated and poorly differentiated components of the metastasis (right panel) (*n*=2). Scale bar: 50 µm. (G) Localization and histological analysis of an extragonadal tumor. Left image shows the tumor mass in the abdominal cavity. The square identifies the area of tumor development within the dorsal mesentery and arrow points to the tumor. Middle panel shows a histological preparation of the tumor, located between the kidneys (asterisk). Dashed square points to a representative enlarged area showing differentiated and poorly differentiated components of the metastasis (right panel) (*n*=1). Scale bar: 50 µm.

Journal of Cell Science (2022) 135, jcs259375. doi:10.1242/jcs.259375

(one male and one female) out 39 *Spo11*^{Cre} *Pten*$^{+/flox}$ *BRaf*^{V600E} mice, we found that the tumor was localized within the dorsal mesentery while the gonads were free of lesions (Fig. 2G).

Prepubertal *Spo11*^{Cre} *Pten*$^{+/flox}$ *BRaf*^{V600E} testes contain tumors at different stages of development

To better understand the kinetics of teratocarcinoma formation, we killed male *Spo11*^{Cre} *Pten*$^{+/flox}$ *BRaf*^{V600E} pups at 7 dpp to check for the presence of the tumor. There were no gross external alterations of the testis in any of the 12 mice examined; however, in two independent testes we were able to find areas of partial tubular atrophy, characterized by the coalescence of multiple seminiferous tubules that contained germ cells with clear cytoplasm and large nuclei (Fig. 3A). Within these areas, small neoplastic islands were found that stained positive for Sox2 and Oct4 (Fig. 3B). We verified whether the molecular pathways activated by *BRaf*^{V600E} mutation with or without *Pten* hemizygous deletion were turned on by performing western blot analysis on isolated mitotic male germ cells at 7 dpp. As shown in Fig. 3B we found that phosphorylated (p)Akt1 levels were upregulated in *Pten*$^{+/-}$ germ cells while pErk (pErk1/2) levels increased only in the presence of the BRaf^{V600E} activation, indicating that spermatogonia were the target cells of dysregulated phosphoinositide 3-kinase (PI3K) or MAPK signaling, and that the two pathways did not cross-talk, as we previously showed following KL stimulation (Dolci et al., 2001). Interestingly, we found that Kit levels were upregulated in *BRaf*^{V600E} and in *Pten*-mutated spermatogonia, suggesting that Kit overexpression together with *de novo* Sox2 expression might represent an important step in the process of gonocyte transformation. We then checked the impact of the different genotypes on spermatogonia proliferation. To this end, we probed testis sections for Ki67 and phosphorated histone 3 (pH3), which unambiguously reported germ cell proliferative activity. As shown in Fig. 3D, we found a significant increase in the proportion of Ki67- and pH3-positive cells in *Spo11*^{Cre} *Pten*$^{+/flox}$ *BRaf*^{V600E}, *Spo11*^{Cre} *BRaf*^{V600E} or *Spo11*^{Cre} *Pten*$^{+/flox}$ testes with respect to control testes. From these results, we speculate that constitutively active MAPK pathway induces Sox2 expression and, concomitantly with the enhancement of proliferation, this can drive germ cell transformation.

BRaf^{V600E}-mutated ovaries contain increased numbers of follicles and metaphase I oocytes

Histological analysis on ovaries contralateral to the tumor or from non-tumoral females at 25 dpp revealed a significant difference in the overall number of follicles per ovarian section when comparing *wt* or *Pten*$^{+/flox}$ versus *BRaf*^{V600E} mutated ovaries.

By counting follicles in hematoxylin and eosin (H&E)-stained sections and anti-Vasa (also known as Ddx4)-positive cells, that corresponded to oocytes, we found that *wt* and *Pten*$^{+/flox}$ mutated ovaries contained similar numbers of primordial, primary and pre-antral follicles, while *Pten*$^{+/flox}$ *BRaf*^{V600E} or *BRaf*^{V600E}-mutated ovaries had almost double the overall follicle content (Fig. 4A,B). Moreover, we found that ovaries from the latter genotypes contained MOFs, mostly at the pre-antral stage (Fig. 4A). In each ovarian sample, MOF numbers ranged from one to five per ovarian section in *BRaf*^{V600E}-mutated genotypes, while we did not detect any MOF in *wt* or *Pten*-mutated ovaries (Table S2). We also found that ovaries from *BRaf*^{V600E}-mutated genotypes also contained metaphase I oocytes (one or two per ovary) with condensed chromosomes at the metaphase plate enclosed by single or multiple layers of follicle cells (Fig. 4A; Fig. S2B), indicating that an overactive MAPK pathway accelerated oocyte maturation. We found that pErk and Kit levels were enhanced in *BRaf*^{V600E}-mutated ovaries compared to control samples (Fig. 4C,D); however, we did not observe any pAkt nor Sox2 increase in *Spo11*^{Cre} *Pten*$^{+/flox}$*BRaf*^{V600E} ovaries (Fig. 4C). To understand whether the increased number of follicles was due to a decrease of oocyte cell death during perinatal life, we counted oocytes showing γH2Ax-positive foci (a marker of DNA damage) in *wt* or *BRaf*^{V600E} mutated ovaries. As shown in Fig. 4E,F, we found that the number of γH2Ax-positive oocytes was increased by about three times in *Spo11*^{Cre} *Pten*$^{+/flox}$ *BRaf*^{V600E} and two times in *Spo11*^{Cre} *BRaf*^{V600E} compared to control oocytes.

DISCUSSION

GCTs represent a model of neoplastic transformation in which the cell of origin ranges from PGCs to gonocytes (De Felici and Dolci, 2013; Dolci et al., 2015); however, the identification of the correct germ cell type is under debate. In particular, it remains to be elucidated if GCNIS, the debuting lesion in males, originates from PGCs or from gonocytes to proceed into more aggressive phenotypes following puberty. A current hypothesis for TGCTs supports the notion that they could derive from hyperproliferative fetal germ cells incompletely determined into the germline (SE) or from fetal germ cells that did not completely repress the pluripotency program (non-SE) (De Felici et al., 2021; Dolci et al., 2015). In humans, the molecular events that drive germ cell transformation have not been fully elucidated yet; however, susceptible loci associated to type I TGCTs have been identified by genome-wide association studies (GWAS), in particular genes related to stemness factors (Litchfield et al., 2016), to PI3K and MAPK signaling (Sasaki et al., 2003) or KIT gain of function mutations (Hersmus et al., 2012; Kemmer et al., 2004). We previously showed that MAPK alone or in combination with the PI3K pathway is essential for the regulation of proliferation in mouse PGCs and spermatogonia (Dolci et al., 1991, 2001; Rossi et al., 1993; Sorrenti et al., 2020; Tassinari et al., 2015), and that the Kit D814Y mutation in embryonic stem cells (ESCs) accelerates EC growth, when transplanted in nude mice (Todaro et al., 2019). In keeping with these results, a recent mouse model (Pierpont et al., 2017) has shown that a double simultaneous event, *Pten* deletion and *Kras*^{G12V} mutation, in fetal male gonocytes, drives mouse germ cell transformation giving rise to EC. To over-activate the germ cell MAPK pathway, we inserted the rarer *BRaf*^{V600E} mutation (Honecker et al., 2009; Meintker et al., 2020), and we found that, independently from *Pten* heterozygosity, the *BRaf*^{V600E} mutation induced gonadal or extragonadal GCTs both in males and in females. By contrast, *Pten* heterozygosity alone never resulted in GCT development, at least up to 5 months after birth (data not shown). The incomplete penetrance of tumor transformation observed in *Spo*^{Cre} *BRaf*^{V600E} *Pten*$^{+/flox}$ mice could depend on the lack of a strong PI3K overactive signaling, as would occur if *Pten* was homozygously deleted. However, since tumorigenesis was observed also in *Spo*^{Cre} *BRaf*^{V600E} mice, this evidence suggested that overactivation of MAPK signaling could be sufficient to drive transformation when germ cells were edited. This hypothesis was corroborated by the observation that the incidence of tumor formation paralleled the frequency of Spo11^{Cre} expression in 12.5 dpc PGCs, as revealed by the *R26-Eyfp* locus editing. Indeed, this result was unexpected, since Spo11 starts to be expressed in early meiotic germ cells of both sexes (Bellani et al., 2010), even though a fetal early-meiotic program has been demonstrated in males for meiotic genes such as *Stra8* (Heaney et al., 2012; Pierpont et al., 2017) and *Scp3* (Di Carlo et al., 2000). Since the timing of endogenous Spo11 and transgenic Spo11-directed Cre expression did not coincide, as shown by EYFP positivity in pre-meiotic PGCs, we can speculate that MAPK and Akt activation occurred in a window of

Journal of Cell Science (2022) 135, jcs259375. doi:10.1242/jcs.259375

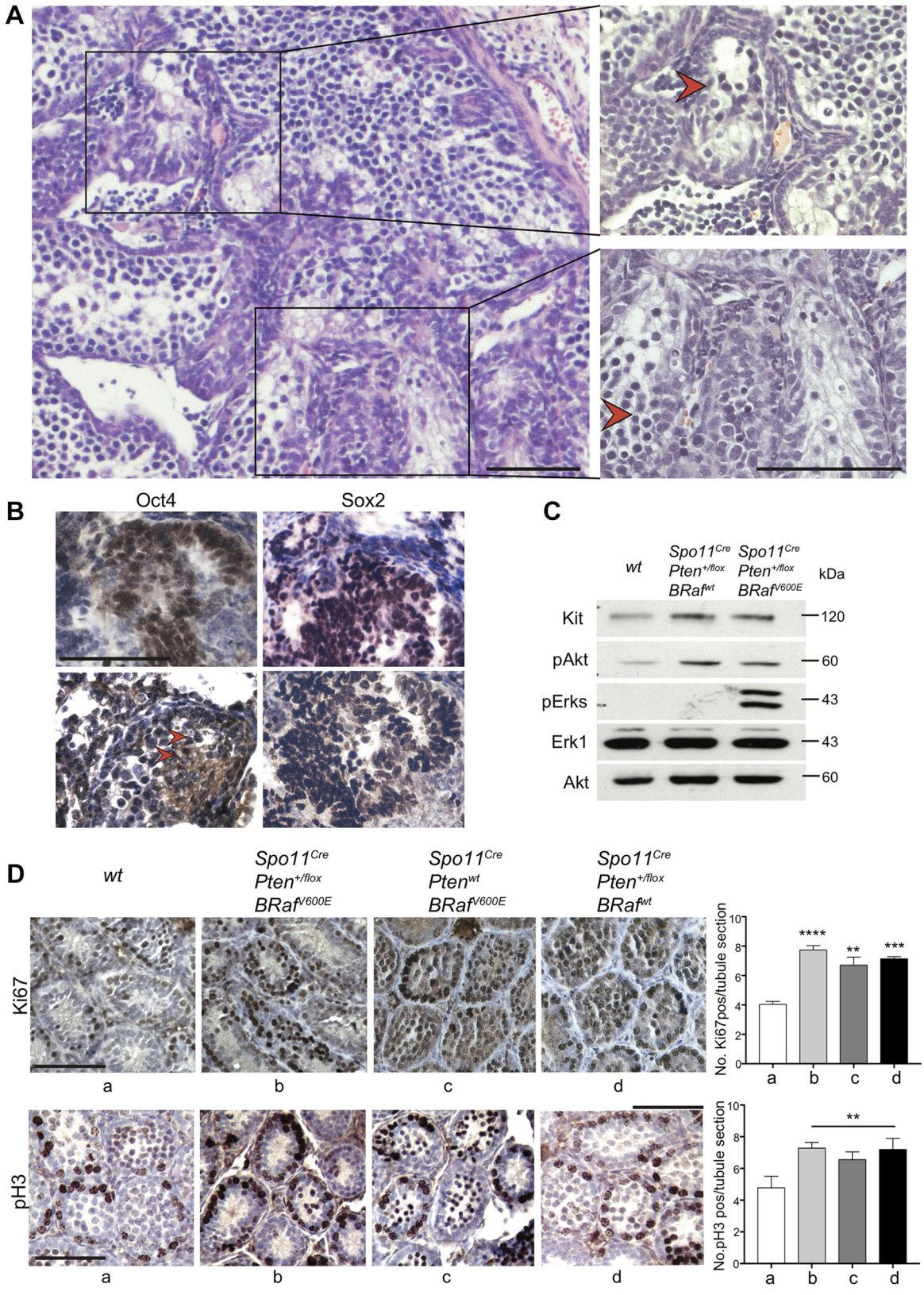

Fig. 3. Germ cell proliferation and tumor transformation in *BRaf*^{V600E} edited male germ cells. (A) Histological analysis of 7 dpp testis showing increased numbers of germ cells containing hyperchromatic nuclei (red arrowheads) and remodeled tubule structure. Dashed squares point to atrophic tubules (n=2). (B) Foci of tumor transformation that stain positive for Oct4 and Sox2. Arrowheads point to Oct4 positive neoplastic germ cells. (n=2). (C) Western blot analysis on isolated mitotic male germ cells at 7 dpp probed for Kit, pAkt and pErks. Erk1 and Akt were used as reference genes (n=3). (D) Immunohistochemical analysis on *Spo11*^{Cre} *Pten*$^{+/flox}$ *BRaf*^{V600E}, *Spo11*^{Cre} *Pten*^{wt} *BRaf*^{V600E}, *Spo11*^{Cre} *Pten*$^{+/flox}$ *BRaf*^{wt} and *wt* mice probed for Ki67 (top) and pH3 (bottom) and relative quantification expressed as percentage of Ki67- or pH3-positive spermatogonia (located at the basal layer of the tubules) per tubule section (top right and bottom right, respectively). Mean±s.d. (n=3, 60 inspected fields). **P<0.01, ***P<0.001, ****P<0.0001 (Welch's t-test). Scale bars: 50 µm.

Journal of Cell Science (2022) 135, jcs259375. doi:10.1242/jcs.259375

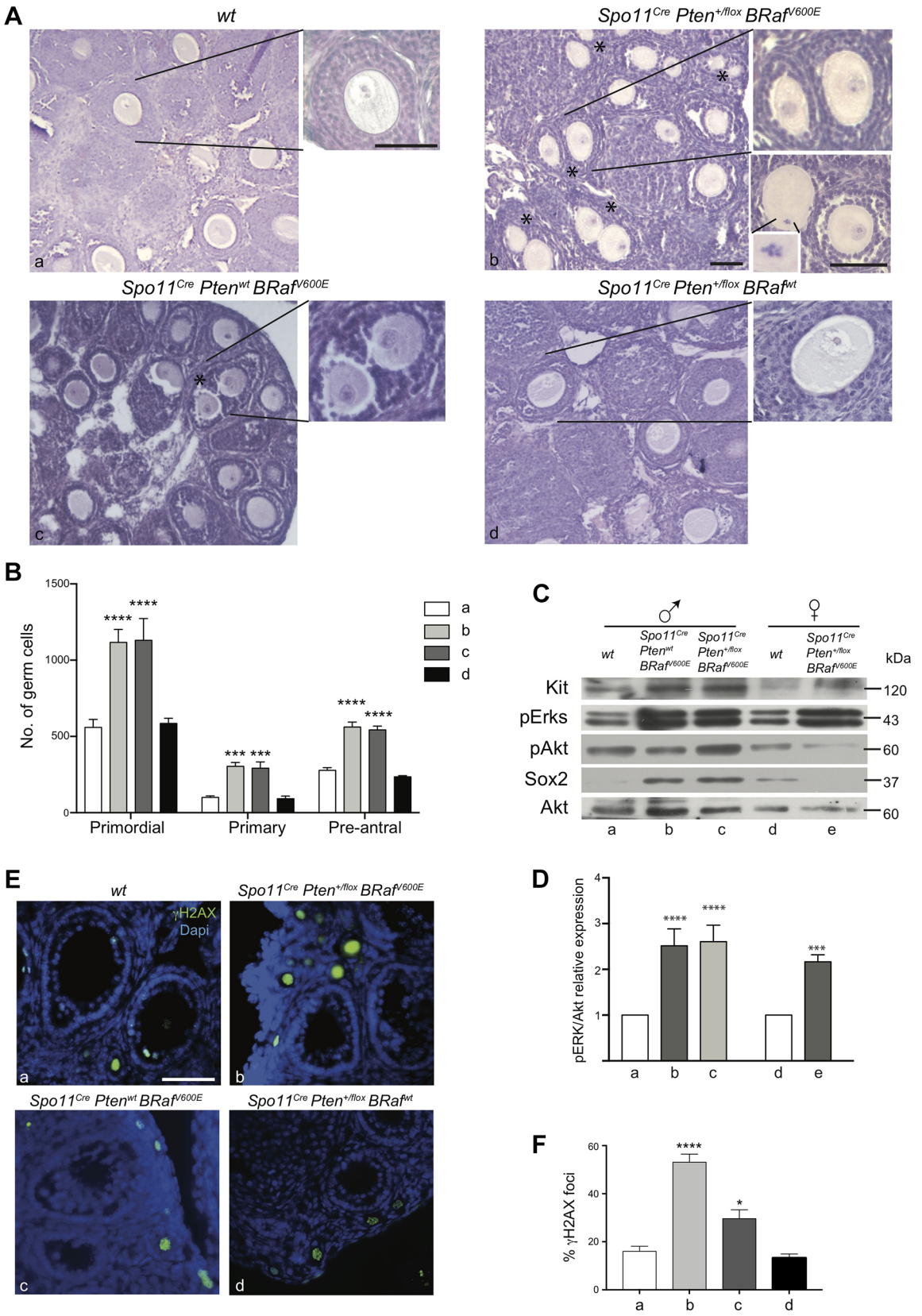

Fig. 4. See next page for legend.

time when germ cells of both sexes are still proliferating. The frequency of tumor formation we found in *BRaf*^{V600E}-only testes differed from that reported by Pierpont et al. (Pierpont et al., 2017), showing that *KRas*^{G12V}-only testes rarely developed testicular tumors. An explanation for this discrepancy might be the different strain used in our study and its relative purity, or alternatively in the

Journal of Cell Science (2022) 135, jcs259375. doi:10.1242/jcs.259375

Fig. 4. Increased numbers of follicles, MOFs and metaphase I-arrested oocytes in *BRaf^{V600E}* edited female germ cells. (A) Histological analysis of *Spo11^{Cre} BRaf^{V600E} Pten$^{+/flox}$*, *Spo11^{Cre} BRaf^{V600E} Pten^{wt}*, *Spo11^{Cre} Pten$^{+/flox}$ BRaf^{wt}* and *wt* ovaries. Magnified areas are from follicles that contain single or multiple oocytes (*). Upper right and lower left panels contain MOFs. Upper right panel also shows a metaphase I follicle enclosed oocyte and the inset shows a fivefold enlargement of metaphase I chromosomes. Scale bars: 50 µm. (B) Histogram representing germ cell number counts in *Spo11^{Cre} Pten$^{+/flox}$ BRaf^{V600E}*, *Spo11^{Cre} Pten^{wt} BRaf^{V600E}*, *Spo11^{Cre} Pten$^{+/flox}$ BRaf^{wt}* and *wt* ovaries. Mean±s.d., (*n*=3). ***P<0.001, ****P<0.0001 (two-way ANOVA with Dunnett's multiple comparisons test). (C) Western blot analysis on *Spo11^{Cre} Pten$^{+/flox}$ BRaf^{V600E}*, *Spo11^{Cre} Pten^{wt} BRaf^{V600E}* and *wt* testis and ovary extracts probed for Kit, pAkt, pErks and Sox2. Akt was used as reference gene (*n*=3). (D) Densitometry of pERK expression normalized on the reference gene (Akt) from blots as shown in C. Mean±s.d. (*n*=3). ***P<0.001, ****P<0.0001 (two-way ANOVA with multiple comparisons test). (E) Immunofluorescence analysis on 25 dpp ovaries probed for γH2Ax (green) and counterstained with DAPI (blue). Scale bars: 50 µm. (*n*=3). (E) Quantitative analysis of γH2Ax foci in oocytes. Mean±s.e.m. (*n*=3, 60 inspected fields). *P<0.05, ****P<0.0001 (Kruskal–Wallis test with Dunn's multiple comparisons test).

ability of the BRaf-activated pathways compared to the KRas-activated pathway to transform germ cells. Histologically, gonadal or extragonadal tumors appeared as teratocarcinomas with areas of differentiated teratomatous tissue and infiltrating undifferentiated EC cells showing Sox2, Oct4, AP2γ and Prdm14 positivity, similar to what is seen in the human counterpart (de Jong et al., 2008; Gell et al., 2018). The tumors were found to metastasize the intestine, indicating that cancer cells possess high invading activity. We never observed tumors at birth in both sexes, but we found initial tumor lesions in prepuberal testes, suggesting that the oncogenic transduction might have occurred perinatally. We found that some cells of initial tumor lesions stained positive for Sox2 and Oct4, while the surrounding differentiated male germ cells were negative. Since Oct4 is expressed in spermatogonia stem cells (Dann et al., 2008), while Sox2 rapidly disappears from PGCs by 13.5 dpc (Campolo et al., 2013), this suggests that re-acquisition of stemness gene expression in edited germ cells is one of the first events that leads to neoplastic transformation. The observation that rare late PGCs clusters showed Spo11^{Cre} activity at 12.5 dpc within the gonads and that extragonadal tumors occurred in both sexes, further suggested that PGCs are the tumor-originating cells. Moreover, the presence of ectopic tumors within the dorsal mesentery indicates that late migratory PGCs, which did not reach the gonads, were the targets of Cre-editing activity in both sexes, thus giving origin to ECs. The presence of initial tumoral lesions in early postnatal testes suggests that edited PGCs can stay silent up to early postnatal life and then can give rise to EC-containing teratomas.

When *Pten* and *Braf^{V600E}* mutations were introduced, Erk and/or PI3K overactivation in premeiotic spermatogonia induced higher proliferative activity compared to *wt* genotypes, as judged by the Ki67 or pH3 positivity of spermatogonia, indicating that the two pathways independently sustain germ cell proliferation.

Non-DGs in humans are rarer tumors compared to testicular ECs (1 in 200,000 females versus 9 in 100,000 males; https://www.orpha.net/consor/cgi-bin/OC_Exp.php?lng=EN&Expert=35807; Znaor et al., 2014) but histologically they resemble their male counterparts (Kurman and Norris, 1976). They are thought to originate from fetal germ cells; however, to date, no mouse model closely recapitulated the disease. *Pten* deletion in PGCs occasionally gives rise to mature teratomas, whereas *Pten* deletion in postnatal oocytes leads to follicular exhaustion and premature ovarian failure (POF) (Reddy et al., 2008). On the other hand, *LT*/*Sv* or *Mos*-null females develop mature or dermoid cyst teratomas that derive from mature oocytes undergoing spontaneous parthenogenetic activation (Hirao and Eppig, 1997a,b).

Our mouse model shows that also female PGCs can undergo transformation, and that MAPK pathway activation is an essential pre-requisite. We found that Spo11^{Cre} expression was present in the majority of fetal and postnatal oocytes in all Spo11^{Cre}-positive ovaries, as judged by β-gal positivity; however, a small fraction of proliferating oogonia had already activated the transgene at ∼12.5 dpc in ∼30% Spo11^{Cre} positive ovaries. As for males, the frequency of such premature Cre expression, shown by EYFP editing, paralleled the frequency of tumor formation. However, as for males, the lack of a co-transforming event cannot be ruled out to explain the reduced penetrance of tumor formation.

Our results also showed that female teratocarcinomas contained pluripotent stem cells possessing invasive activity that metastasized the surrounding intestinal loops. MAPK pathway overactivation in meiotic oocytes led to an increased number of primordial, primary and pre-antral follicles, reminiscent of what previously observed in *Bax*-deleted ovaries (Perez et al., 1999). Indeed, increased numbers of follicle enclosed oocytes showing γH2Ax-positive foci were found in *Spo^{Cre} BRaf^{V600E}*-containing genotypes, suggesting that they did not undergo apoptosis and survived beyond the pachytene

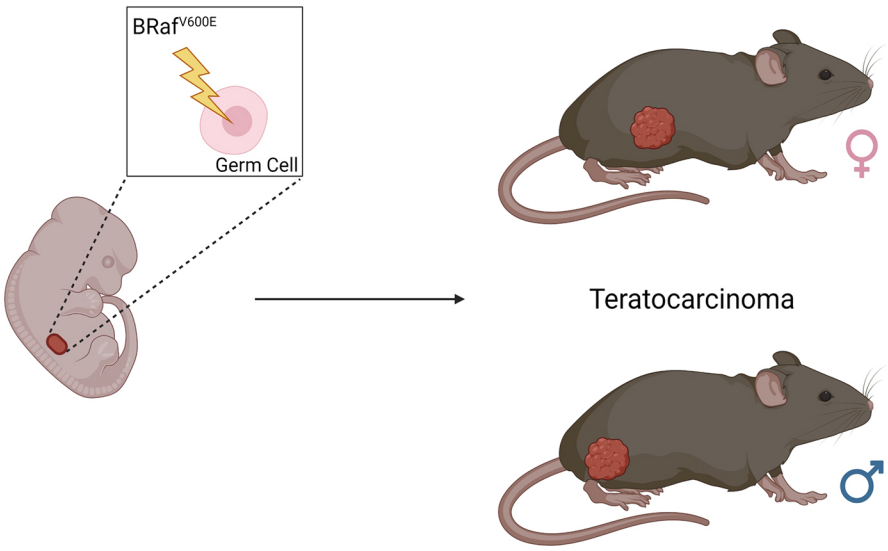

Fig. 5. Graphical representation of the proposed mouse model of BRaf^{V600E}-driven tumorigenesis in male and female late PGCs.

checkpoint, after birth. Moreover, all activatable *BRaf*^{V600E} genotypes developed MOFs and a fraction of oocytes was found arrested at metaphase I. MOFs are thought to derive from oocyte cysts that do not undergo complete breakdown (Jefferson et al., 2000), and multiple genes from granulosa cells or oocytes affect such process. Our results suggest that sustained MAPK activation in oocytes can modify oocyte–granulosa cell communication, leading to follicle formation anomalies. Finally, the presence of metaphase I-arrested oocytes in *BRaf*^{V600E}-mutated ovaries demonstrates for the first time that overactivation of MAPK pathway specifically in oocytes leads to meiotic G2-M transition *in vivo* in the absence of hormonal stimulation and oocyte ovulation.

In conclusion, our results suggest that activation of *BRaf*^{V600E} mutation in late PGCs can lead to male or female germ cell transformation (Fig. 5). Its overactivity at later stages of germ cell development can: (1) expand the mitotic germ cell pool in males and the follicular pool in females, (2) affect follicle formation and (3) accelerate meiotic maturation of fully grown oocytes, independently from granulosa cells and hormonal stimulation.

MATERIALS AND METHODS

Mice and genotyping procedures

Pten$^{flox/flox}$ (Dankort et al., 2009) *BRaf*^{V600E} mice were obtained from Jackson Laboratories and are as previously described (Dankort et al., 2009). *Spo11*^{Cre} mice, previously described in Pellegrini et al. (2011), were intercrossed and progeny was *Spo11*^{Cre} genotyped.*LacZ-R26*$^{flox/flox}$ and *Eyfp-R26*$^{flox/flox}$ mice were kindly provided by GianGiacomo Consalez (University of San Raffaele, Milan Italy). Primers used for genotyping are reported in Table S3.

DNA was extracted from tails using proteinase K (P2308, Sigma-Aldrich, Darmstadt, Germany); template amplification was performed using MyTaq Red Mix (BIO-25044, Meridian Bioscience, Cincinnati, Ohio, USA). For staging embryos, 0.5 days post coitum (dpc) corresponded to the day of vaginal plug.

All experimental procedures involving mice were approved by the Italian Ministry of Health and were performed according to the guidelines of the Stazione per la Tecnologia Animale – University of Rome Tor Vergata.

Histology, immunohistochemistry and immunofluorescence

H&E staining and immunohistochemistry analysis were performed onto 4% formalin-fixed, paraffin-embedded sections (5 µm) mounted on positively charged glass slides. Human GCTs sections were obtained from routine pathology evaluations at Sant'Eugenio Hospital (Rome, Italy), according to the local ethics committee, after receiving informed consent of the patients. All investigations were performed according to the principles expressed in the Declaration of Helsinki.

For immunohistochemistry, sections were incubated overnight at 4°C with primary antibody diluted in DAKO ChemMate^{TM} Antibody Diluent, extensively washed in PBS, incubated for 1 h at room temperature with peroxidase-conjugated secondary antibodies and then revealed by DAB substrate (Dako). Sections were then counterstained with hematoxylin.

For immunofluorescence analysis on tissue samples, antigen retrieval was performed incubating sections with sodium citrate and primary antibodies were incubated overnight. Secondary antibodies and DAPI were purchased from Thermo Fisher (Monza, Italy).

Positive control immunolocalizations for Oct4, Sox2, Prdm14, AP2γ, Ki67, pH3 and γH2Ax were run on testicular sections of 12.5 dpc testes (not shown) while negative control immunolocalizations were performed on testicular sections omitting the primary antibody (not shown).

For β-galactosidase staining, embryos and tissues were processed as previously described (Zappone et al., 2000).

Counts on follicles were performed as described by Ratts et al. Briefly, paraffin-embedded ovaries were sectioned, and every fifth section was stained with H&E and analyzed for total number of oocytes. Counts were performed on a total of 10 sections, analyzing 60 fields per genotype (Ratts et al., 1995).

Primary antibodies used are listed in Table S4.

Western blotting

For western blotting analysis, membranes were incubated overnight with primary antibodies at 4°C. The horseradish-peroxidase-conjugated secondary antibodies (m-IgGκ, sc-516102, and mouse anti-rabbit-IgG, sc-2357; Santa Cruz Biotechnologies, Dallas, Texas, USA) were incubated 1 h at room temperature and revealed by chemiluminescence (Bio-Rad, Hercules, California, USA).

Full original blots are shown in Fig. S3, and primary antibodies used are listed in Table S4.

Statistical analysis

All analyses were performed with Prism 7 software. Results are shown as mean±s.d. or mean±s.e.m. Statistical tests were considered significant for relative values $P<0.05$. All experiments were performed on at least three biological replicates. Male mice of up to 5 months in age were used for analysis of TGCT formation.

Acknowledgements

We thank G. G. Consalez (University of San Raffaele, Milan Italy), for sharing *LacZ-R26*$^{flox/flox}$ and *Eyfp-R26*$^{flox/flox}$ mice were. We also thank Mrs M. Paglialunga, S. Pucci and Mr F. Lancia for animal husbandry.

Competing interests

The authors declare no competing or financial interests.

Author contributions

Conceptualization: E.G., V.T., S.D.; Methodology: E.G., V.T., A.C., F.T., V.C., B.G.J., F.B., G.R.; Software: P.R.; Validation: E.G., V.T., A.C.; Investigation: E.G., V.T., A.C., F.T.; Resources: M.P., F.B.; Writing - review & editing: E.G., V.T., P.R., E.A.J.; Supervision: S.D.; Funding acquisition: E.A.J., S.D.

Funding

S.D. was supported by Progetti di Rilevante Interesse Nazionale (PRIN) grant #2017ATZ2YK_002. E.A.J. was supported by PRIN grant #2017S9KTNE_002.

Peer review history

The peer review history is available online at https://journals.biologists.com/jcs/article-lookup/doi/10.1242/jcs.259375.

References

Bellani, M. A., Boateng, K. A., McLeod, D. and Camerini-Otero, R. D. (2010). The expression profile of the major mouse SPO11 isoforms indicates that SPO11β introduces double strand breaks and suggests that SPO11alpha has an additional role in prophase in both spermatocytes and oocytes. *Mol. Cell. Biol.* **30**, 4391-4403. doi:10.1128/MCB.00002-10

Bosl, G. J. and Motzer, R. J. (1997). Testicular germ-cell cancer. *N. Engl. J. Med.* **337**, 242-254. doi:10.1056/NEJM199707243370406

Boublikova, L., Bakardjieva-Mihaylova, V., Skvarova Kramarzova, K., Kuzilkova, D., Dobiasova, A., Fiser, K., Stuchly, J., Kotrova, M., Buchler, T., Dusek, P., et al. (2016). Wilms tumor gene 1 (WT1), TP53, RAS/BRAF and KIT aberrations in testicular germ cell tumors. *Cancer Lett.* **376**, 367-376. doi:10.1016/j.canlet.2016.04.016

Campolo, F., Gori, M., Favaro, R., Nicolis, S., Pellegrini, M., Botti, F., Rossi, P., Jannini, E. A. and Dolci, S. (2013). Essential role of Sox2 for the establishment and maintenance of the germ cell line. *Stem Cells* **31**, 1408-1421. doi:10.1002/stem.1392

Dankort, D., Curley, D. P., Cartlidge, R. A., Nelson, B., Karnezis, A. N., Damsky, W. E., Jr, You, M. J., DePinho, R. A., McMahon, M. and Bosenberg, M. (2009). Braf(V600E) cooperates with Pten loss to induce metastatic melanoma. *Nat. Genet.* **41**, 544-552. doi:10.1038/ng.356

Dann, C. T., Alvarado, A. L., Molyneux, L. A., Denard, B. S., Garbers, D. L. and Porteus, M. H. (2008). Spermatogonial stem cell self-renewal requires OCT4, a factor downregulated during retinoic acid-induced differentiation. *Stem Cells* **26**, 2928-2937. doi:10.1634/stemcells.2008-0134

De Felici, M. and Dolci, S. (2013). From testis to teratomas: a brief history of male germ cells in mammals. *Int. J. Dev. Biol.* **57**, 115-121. doi:10.1387/ijdb.130069md

De Felici, M., Klinger, F. G., Campolo, F., Balistreri, C. R., Barchi, M. and Dolci, S. (2021). To be or not to be a germ cell: the extragonadal germ cell tumor paradigm. *Int. J. Mol. Sci.* **22**, 5982. doi:10.3390/ijms22115982

de Jong, J., Stoop, H., Gillis, A. J., van Gurp, R. J., van de Geijn, G. J., Boer, M., Hersmus, R., Saunders, P. T., Anderson, R. A., Oosterhuis, J. W., et al.

(2008). Differential expression of SOX17 and SOX2 in germ cells and stem cells has biological and clinical implications. *J. Pathol.* **215**, 21-30. doi:10.1002/path.2332

Depue, R. H., Pike, M. C. and Henderson, B. E. (1983). Estrogen exposure during gestation and risk of testicular cancer. *J. Natl. Cancer Inst.* **71**, 1151-1155.

Di Carlo, A. D., Travia, G. and De Felici, M. (2000). The meiotic specific synaptonemal complex protein SCP3 is expressed by female and male primordial germ cells of the mouse embryo. *Int. J. Dev. Biol.* **44**, 241-244.

Dolci, S., Williams, D. E., Ernst, M. K., Resnick, J. L., Brannan, C. I., Lock, L. F., Lyman, S. D., Boswell, H. S. and Donovan, P. J. (1991). Requirement for mast cell growth factor for primordial germ cell survival in culture. *Nature* **352**, 809-811. doi:10.1038/352809a0

Dolci, S., Pellegrini, M., Di Agostino, S., Geremia, R. and Rossi, P. (2001). Signaling through extracellular signal-regulated kinase is required for spermatogonial proliferative response to stem cell factor. *J. Biol. Chem.* **276**, 40225-40233. doi:10.1074/jbc.M105143200

Dolci, S., Campolo, F. and De Felici, M. (2015). Gonadal development and germ cell tumors in mouse and humans. *Semin. Cell Dev. Biol.* **45**, 114-123. doi:10.1016/j.semcdb.2015.10.002

Feldman, D. R., Voss, M. H., Jacobsen, E. P., Jia, X., Suarez, J. A., Turkula, S., Sheinfeld, J., Bosl, G. J., Motzer, R. J. and Patil, S. (2013). Clinical features, presentation, and tolerance of platinum-based chemotherapy in germ cell tumor patients 50 years of age and older. *Cancer* **119**, 2574-2581. doi:10.1002/cncr.28025

Feldman, D. R., Iyer, G., Van Alstine, L., Patil, S., Al-Ahmadie, H., Reuter, V. E., Bosl, G. J., Chaganti, R. S. and Solit, D. B. (2014). Presence of somatic mutations within PIK3CA, AKT, RAS, and FGFR3 but not BRAF in cisplatin-resistant germ cell tumors. *Clin. Cancer Res.* **20**, 3712-3720. doi:10.1158/1078-0432.CCR-13-2868

Gell, J. J., Zhao, J., Chen, D., Hunt, T. J. and Clark, A. T. (2018). PRDM14 is expressed in germ cell tumors with constitutive overexpression altering human germline differentiation and proliferation. *Stem Cell Res* **27**, 46-56. doi:10.1016/j.scr.2017.12.016

Gershenson, D. M. (2007). Management of ovarian germ cell tumors. *J. Clin. Oncol.* **25**, 2938-2943. doi:10.1200/JCO.2007.10.8738

Heaney, J. D., Anderson, E. L., Michelson, M. V., Zechel, J. L., Conrad, P. A., Page, D. C. and Nadeau, J. H. (2012). Germ cell pluripotency, premature differentiation and susceptibility to testicular teratomas in mice. *Development* **139**, 1577-1586. doi:10.1242/dev.076851

Hersmus, R., Stoop, H., van de Geijn, G. J., Eini, R., Biermann, K., Oosterhuis, J. W., Dhooge, C., Schneider, D. T., Meijssen, I. C., Dinjens, W. N., et al. (2012). Prevalence of c-KIT mutations in gonadoblastoma and dysgerminomas of patients with disorders of sex development (DSD) and ovarian dysgerminomas. *PLoS One* **7**, e43952. doi:10.1371/journal.pone.0043952

Hirao, Y. and Eppig, J. J. (1997a). Analysis of the mechanism(s) of metaphase I arrest in strain LT mouse oocytes: participation of MOS. *Development* **124**, 5107-5113. doi:10.1242/dev.124.24.5107

Hirao, Y. and Eppig, J. J. (1997b). Parthenogenetic development of Mos-deficient mouse oocytes. *Mol. Reprod. Dev.* **48**, 391-396. doi:10.1002/(SICI)1098-2795(199711)48:3<391::AID-MRD13>3.0.CO;2-Z

Honecker, F., Wermann, H., Mayer, F., Gillis, A. J., Stoop, H., van Gurp, R. J., Oechsle, K., Steyerberg, E., Hartmann, J. T., Dinjens, W. N., et al. (2009). Microsatellite instability, mismatch repair deficiency, and BRAF mutation in treatment-resistant germ cell tumors. *J. Clin. Oncol.* **27**, 2129-2136. doi:10.1200/JCO.2008.18.8623

Jefferson, W. N., Couse, J. F., Banks, E. P., Korach, K. S. and Newbold, R. R. (2000). Expression of estrogen receptor β is developmentally regulated in reproductive tissues of male and female mice. *Biol. Reprod.* **62**, 310-317. doi:10.1095/biolreprod62.2.310

Kemmer, K., Corless, C. L., Fletcher, J. A., McGreevey, L., Haley, A., Griffith, D., Cummings, O. W., Wait, C., Town, A. and Heinrich, M. C. (2004). KIT mutations are common in testicular seminomas. *Am. J. Pathol.* **164**, 305-313. doi:10.1016/S0002-9440(10)63120-3

Kimura, T., Suzuki, A., Fujita, Y., Yomogida, K., Lomeli, H., Asada, N., Ikeuchi, M., Nagy, A., Mak, T. W. and Nakano, T. (2003). Conditional loss of PTEN leads to testicular teratoma and enhances embryonic germ cell production. *Development* **130**, 1691-1700. doi:10.1242/dev.00392

Krentz, A. D., Murphy, M. W., Kim, S., Cook, M. S., Capel, B., Zhu, R., Matin, A., Sarver, A. L., Parker, K. L., Griswold, M. D., et al. (2009). The DM domain protein DMRT1 is a dose-sensitive regulator of fetal germ cell proliferation and pluripotency. *Proc. Natl. Acad. Sci. USA* **106**, 22323-22328. doi:10.1073/pnas.0905431106

Kurman, R. J. and Norris, H. J. (1976). Embryonal carcinoma of the ovary. A clinicopathologic entity distinct from endodermal sinus tumor resembling embryonal carcinoma of the adult testis. *Cancer* **38**, 2420-2433. doi:10.1002/1097-0142(197612)38:6<2420::AID-CNCR2820380630>3.0.CO;2-2

Litchfield, K., Levy, M., Huddart, R. A., Shipley, J. and Turnbull, C. (2016). The genomic landscape of testicular germ cell tumours: from susceptibility to treatment. *Nat. Rev. Urol.* **13**, 409-419. doi:10.1038/nrurol.2016.107

Meintker, L., Haller, F., Tögel, L., Schmidt, D., Waibel, H., Hartmann, A., Mackensen, A. and Meidenbauer, N. (2020). Successful targeting of BRAF V600E mutation with vemurafenib in a treatment-resistant extragonadal nonseminomatous germ-cell tumor. *JCO Precis. Oncol.* **4**, 233-238. doi:10.1200/PO.19.00377

Meng, X., de Rooij, D. G., Westerdahl, K., Saarma, M. and Sariola, H. (2001). Promotion of seminomatous tumors by targeted overexpression of glial cell line-derived neurotrophic factor in mouse testis. *Cancer Res.* **61**, 3267-3271.

Moch, H., Cubilla, A. L., Humphrey, P. A., Reuter, V. E. and Ulbright, T. M. (2016). The 2016 WHO classification of tumours of the urinary system and male genital organs-part A: renal, penile, and testicular tumours. *Eur. Urol.* **70**, 93-105. doi:10.1016/j.eururo.2016.02.029

Oosterhuis, J. W. and Looijenga, L. H. (2005). Testicular germ-cell tumours in a broader perspective. *Nat. Rev. Cancer* **5**, 210-222. doi:10.1038/nrc1568

Pellegrini, M., Claps, G., Orlova, V. V., Barrios, F., Dolci, S., Geremia, R., Rossi, P., Rossi, G., Arnold, B., Chavakis, T., et al. (2011). Targeted JAM-C deletion in germ cells by Spo11-controlled Cre recombinase. *J. Cell Sci.* **124**, 91-99. doi:10.1242/jcs.072959

Perez, G. I., Robles, R., Knudson, C. M., Flaws, J. A., Korsmeyer, S. J. and Tilly, J. L. (1999). Prolongation of ovarian lifespan into advanced chronological age by Bax-deficiency. *Nat. Genet.* **21**, 200-203. doi:10.1038/5985

Permuth-Wey, J. and Sellers, T. A. (2009). Epidemiology of ovarian cancer. *Methods Mol. Biol.* **472**, 413-437. doi:10.1007/978-1-60327-492-0_20

Pierpont, T. M., Lyndaker, A. M., Anderson, C. M., Jin, Q., Moore, E. S., Roden, J. L., Braxton, A., Bagepalli, L., Kataria, N., Hu, H. Z., et al. (2017). Chemotherapy-induced depletion of OCT4-positive cancer stem cells in a mouse model of malignant testicular cancer. *Cell Rep* **21**, 1896-1909. doi:10.1016/j.celrep.2017.10.078

Quirk, J. T., Natarajan, N. and Mettlin, C. J. (2005). Age-specific ovarian cancer incidence rate patterns in the United States. *Gynecol. Oncol.* **99**, 248-250. doi:10.1016/j.ygyno.2005.06.052

Rajpert-De Meyts, E. (2006). Developmental model for the pathogenesis of testicular carcinoma in situ: genetic and environmental aspects. *Hum. Reprod. Update* **12**, 303-323. doi:10.1093/humupd/dmk006

Ratts, V. S., Flaws, J. A., Kolp, R., Sorenson, C. M. and Tilly, J. L. (1995). Ablation of bcl-2 gene expression decreases the numbers of oocytes and primordial follicles established in the post-natal female mouse gonad. *Endocrinology* **136**, 3665-3668. doi:10.1210/endo.136.8.7628407

Reddy, P., Liu, L., Adhikari, D., Jagarlamudi, K., Rajareddy, S., Shen, Y., Du, C., Tang, W., Hamalainen, T., Peng, S. L., et al. (2008). Oocyte-specific deletion of Pten causes premature activation of the primordial follicle pool. *Science* **319**, 611-613. doi:10.1126/science.1152257

Reuter, V. E. (2005). Origins and molecular biology of testicular germ cell tumors. *Mod. Pathol.* **18** Suppl. 2, S51-S60. doi:10.1038/modpathol.3800309

Rossi, P., Dolci, S., Albanesi, C., Grimaldi, P., Ricca, R. and Geremia, R. (1993). Follicle-stimulating hormone induction of steel factor (SLF) mRNA in mouse Sertoli cells and stimulation of DNA synthesis in spermatogonia by soluble SLF. *Dev. Biol.* **155**, 68-74. doi:10.1006/dbio.1993.1007

Sasaki, A., Taketomi, T., Kato, R., Saeki, K., Nonami, A., Sasaki, M., Kuriyama, M., Saito, N., Shibuya, M. and Yoshimura, A. (2003). Mammalian Sprouty4 suppresses Ras-independent ERK activation by binding to Raf1. *Nat. Cell Biol.* **5**, 427-432. doi:10.1038/ncb978

Skakkebaek, N. E., Berthelsen, J. G., Giwercman, A. and Müller, J. (1987). Carcinoma-*in-situ* of the testis: possible origin from gonocytes and precursor of all types of germ cell tumours except spermatocytoma. *Int. J. Androl.* **10**, 19-28. doi:10.1111/j.1365-2605.1987.tb00161.x

Sommerer, F., Hengge, U. R., Markwarth, A., Vomschloss, S., Stolzenburg, J. U., Wittekind, C. and Tannapfel, A. (2005). Mutations of BRAF and RAS are rare events in germ cell tumours. *Int. J. Cancer* **113**, 329-335. doi:10.1002/ijc.20567

Sonne, S. B., Almstrup, K., Dalgaard, M., Juncker, A. S., Edsgard, D., Ruban, L., Harrison, N. J., Schwager, C., Abdollahi, A., Huber, P. E., et al. (2009). Analysis of gene expression profiles of microdissected cell populations indicates that testicular carcinoma in situ is an arrested gonocyte. *Cancer Res.* **69**, 5241-5250. doi:10.1158/0008-5472.CAN-08-4554

Sorrenti, M., Klinger, F. G., Iona, S., Rossi, V., Marcozzi, S. and DE Felici, M. (2020). Expression and possible roles of extracellular signal-related kinases 1-2 (ERK1-2) in mouse primordial germ cell development. *J. Reprod. Dev.* **66**, 399-409. doi:10.1262/jrd.2019-141

Stevens, L. C. (1964). Experimental production of testicular teratomas in mice. *Proc. Natl. Acad. Sci. USA* **52**, 654-661. doi:10.1073/pnas.52.3.654

Suzuki, A., de la Pompa, J. L., Stambolic, V., Elia, A. J., Sasaki, T., del Barco Barrantes, I., Ho, A., Wakeham, A., Itie, A., Khoo, W., et al. (1998). High cancer susceptibility and embryonic lethality associated with mutation of the PTEN tumor suppressor gene in mice. *Curr. Biol.* **8**, 1169-1178. doi:10.1016/S0960-9822(07)00488-5

Tassinari, V., Campolo, F., Cesarini, V., Todaro, F., Dolci, S. and Rossi, P. (2015). Fgf9 inhibition of meiotic differentiation in spermatogonia is mediated by

Erk-dependent activation of Nodal-Smad2/3 signaling and is antagonized by Kit Ligand. *Cell Death Dis.* **6**, e1688. doi:10.1038/cddis.2015.56

Todaro, F., Campolo, F., Barrios, F., Pellegrini, M., Di Cesare, S., Tessarollo, L., Rossi, P., Jannini, E. A. and Dolci, S. (2019). Regulation of kit expression in early mouse embryos and ES cells. *Stem Cells* **37**, 332-344. doi:10.1002/stem.2960

Youngren, K. K., Coveney, D., Peng, X., Bhattacharya, C., Schmidt, L. S., Nickerson, M. L., Lamb, B. T., Deng, J. M., Behringer, R. R., Capel, B., et al. (2005). The Ter mutation in the dead end gene causes germ cell loss and testicular germ cell tumours. *Nature* **435**, 360-364. doi:10.1038/nature03595

Zappone, M. V., Galli, R., Catena, R., Meani, N., De Biasi, S., Mattei, E., Tiveron, C., Vescovi, A. L., Lovell-Badge, R., Ottolenghi, S., et al. (2000). Sox2 regulatory sequences direct expression of a (beta)-geo transgene to telencephalic neural stem cells and precursors of the mouse embryo, revealing regionalization of gene expression in CNS stem cells. *Development* **127**, 2367-2382. doi:10.1242/dev.127.11.2367

Znaor, A., Lortet-Tieulent, J., Jemal, A. and Bray, F. (2014). International variations and trends in testicular cancer incidence and mortality. *Eur. Urol.* **65**, 1095-1106. doi:10.1016/j.eururo.2013.11.004